National
Optical
Astronomy
Observatories

National Solar Observatory

Global Oscillation Network Group

Report Number 15

SOLAR MODEL

HARE AND HOUNDS

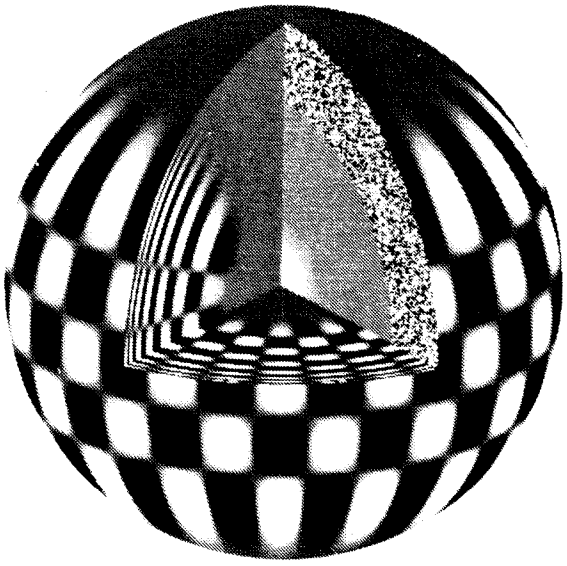

9/25/96

REPORT ON THE STRUCTURE INVERSION HARE-AND-HOUNDS EXERCISE

H.M. Antia[1], S. Basu[2], J. Christensen-Dalsgaard[2,3], J.R. Elliott[4], D.O. Gough[4], J.A. Guzik[5], and A.G. Kosovichev[6]

[1]Tata Institute for Fundamental Research, Mumbai;

[2]Theoretical Astrophysics Centre, Aarhus University;

[3]Theoretical Astrophysics Center, Danish National Research Foundation;

[4]Institute of Astronomy, University of Cambridge;

[5]Los Alamos National Laboratory, New Mexico;

[6]Stanford University

1 Introduction

During the work on inferring the internal structure of the Sun from the initial GONG data, it was decided to carry out a hare-and-hounds exercise to uncover possible uncertainties in the inversion results, and to test the reliability of the error estimates. The exercise was designed to test the 1-D inversions for the spherically symmetrical component of the solar structure. The previous hare-and-hounds exercises dealt with the angular-velocity inversions (see GONG Newsletter 9 and GONG Report 11).

There are several specific features of the structure inversions, which make the inferences about the solar structure more complicated and more subject to additional constraints and prejudices of inversion procedures than the inferences about solar rotation. First, the seismic structure of the Sun is generally determined by, at least, two independent unknown functions of radius r, e.g. density $\rho(r)$ and the adiabatic exponent $\gamma(r)$. Therefore, it is necessary to disentangle the contributions of the unknown functions to the frequency variations of the normal modes. Second, the equations that relate the normal-mode frequencies to the structure variables are generally non-linear, and have to be solved by iterations. Typically, only one iteration of a standard solar model is required for the model to agree with the observed frequencies within the estimated errors. However, the new high-precision frequency measurements from GONG and SOHO will require more iterations. Third, the structure inversions are affected by poorly understood non-adiabatic effects in the upper convective boundary layer. A reliable theoretical description of the effects is not yet available. The standard approach

currently used by most inverters is to approximate the non-adiabatic frequency perturbations by a smooth function of frequency. How accurate this approximation is has not yet been established. Fourth, inversions for the structural properties other than the 'primary' seismic parameters (pressure, density and the adiabatic exponent, and their combinations) inevitably involve theoretical models of the microscopic physics, such as the equation of state, radiative opacity, and nuclear reaction rates, in addition to the basic assumption about the solar structure, hydrostatic equilibrium. Therefore, the inferences about the 'secondary' structure properties (e.g. the helium abundance and the temperature) are sensitive to the uncertainties of the microscopic models. However, in principle, helioseismic inversions may test the microscopic models. All these specific features of structure inversion must be properly addressed in order to draw robust conclusions about the internal structure of the Sun.

The hare-and-hounds exercise was primarily concerned with the determination of the primary seismic variables and possible cross-talk between them, and also with the spatial resolution and error estimates of the inversions. Some secondary inversions have been also carried out. The mode set consisted of low- and intermediate degree p-modes ($l = 0 - 150; \nu = 1.5 - 3$ mHz) confidently measured from the GONG data. The same mode set was used in the first GONG publication (Gough, *et al.*, 1996). The random errors added to the theoretical frequencies were consistent with the errors estimated from the GONG data.

2 Solar Models

The solar model used as the Sun's proxy was computed by J.A. Guzik under the standard assumptions about the solar evolution (Guzik, Cox & Swenson, 1996). The model age was 4.54 Gyr; it included gravitational settling and diffusion of helium and heavier elements as described by Cox, Guzik and Kidman (1989). The authors used the full treatment of Burgers (1969), and solved the coupled equations of diffusion, heat flow, no net mass flow, and no net charge flow for H, ^{3}He, ^{4}He, ^{12}C, ^{14}N, ^{16}O, ^{18}O, Ne, Mg, and the electron. The nuclear reaction rates were taken from the tables by Caughlan and Fowler (1988). The opacity coefficient and the equation of state were computed using the OPAL tables (Rogers and Iglesias, 1992). The initial abundances of helium, Y, and heavy element, Z, were 0.2740 and 0.0195, respectively. The model chosen for the Sun's proxy had small perturbations of the abundances added after the model evolution was completed. The perturbed model was properly calibrated. The distributions of the abundances in the model are shown in Figures 1 and 2.

The solar model used as a reference for the exercise was Model S (Christensen-Dalsgaard *et al.*, 1996), which was also used for the inversion of the initial GONG frequencies. This model was also computed under the standard assumption of the solar evolution, but using a different numerical procedure and different microscopic data. The opacity coefficient and the equation of state were taken from the same

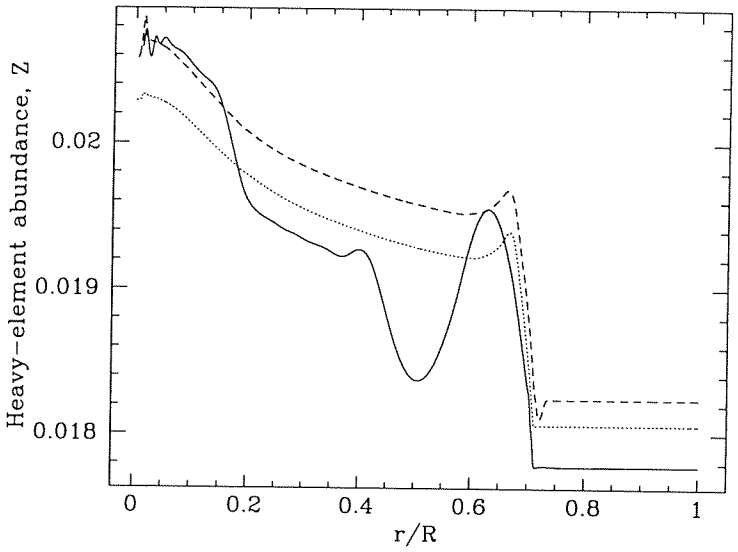

Figure 1: The abundance of heavy elements of the reference solar model by Christensen-Dalsgaard *et al.* (1996) (dotted curve), of the standard solar model by Guzik *et al.* (1996) (dashed curve), and of the perturbed Guzik model used in a proxy Sun (solid curve).

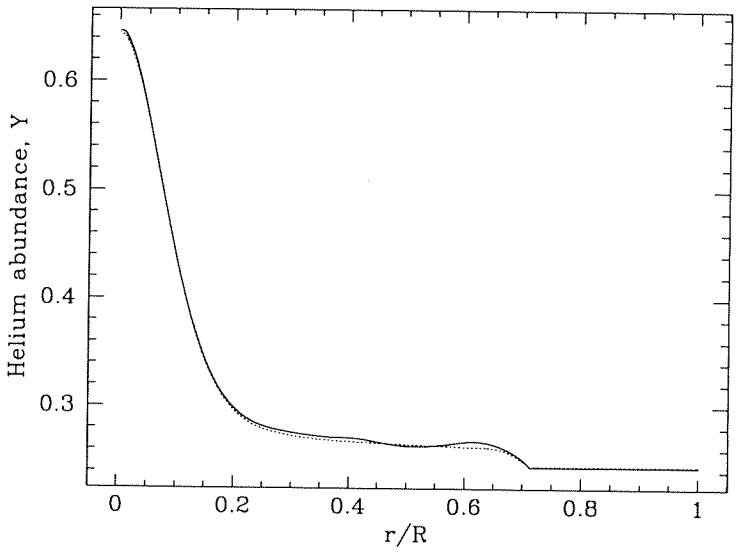

Figure 2: The helium abundance of the proxy Sun (solid curve) and of the reference model (dots).

OPAL tables. However, the interpolation scheme was different from the interpolation used for the proxy. The nuclear reaction parameters were adopted from Bahcall and Pinsonneault (1995). Helium and heavy-element (at the oxygen rates) settling was included, using Michaud and Proffitt's (1993) theory. The initial helium and heavy-element abundances were 0.2713 and 0.01963. The distribution of the abundances in the model after 4.6 Gyr of evolution on the Main Sequence is shown in Figures 1 and 2 by dots.

We note that the seismic characteristics of the proxy and the reference model differ from each other by approximately the same amount as they differ from the real Sun. The relative differences of the sound speed, density, and the adiabatic exponent between the models are shown in Fig. 3.

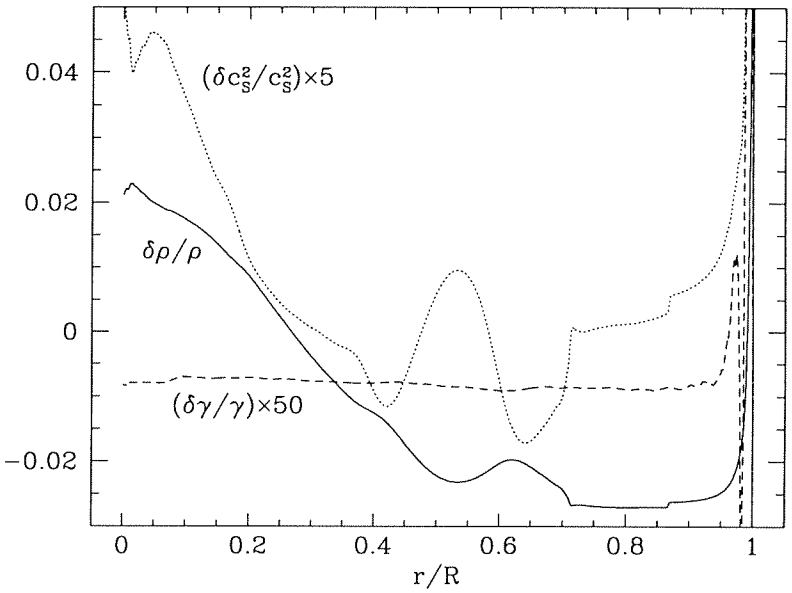

Figure 3: The relative difference of the density, ρ, (solid curve), the sound speed, c_S^2, (dots), and the adiabatic exponent, γ, (dashed curve) between the reference model and the proxy. The variations of the sound speed and the adiabatic exponent are magnified by the factors 5 and 50, respectively.

3 Frequencies

The oscillation frequencies were computed in the adiabatic approximation by A.G. Kosovichev. The upper boundary condition applied at the highest points of the solar models was to match the wave solution in the isothermal atmosphere (Unno *et al.*, 1989). The numerical accuracy of the frequencies estimated from the variational principle (assuming that the pressure perturbation is zero at the upper boundary) is of the

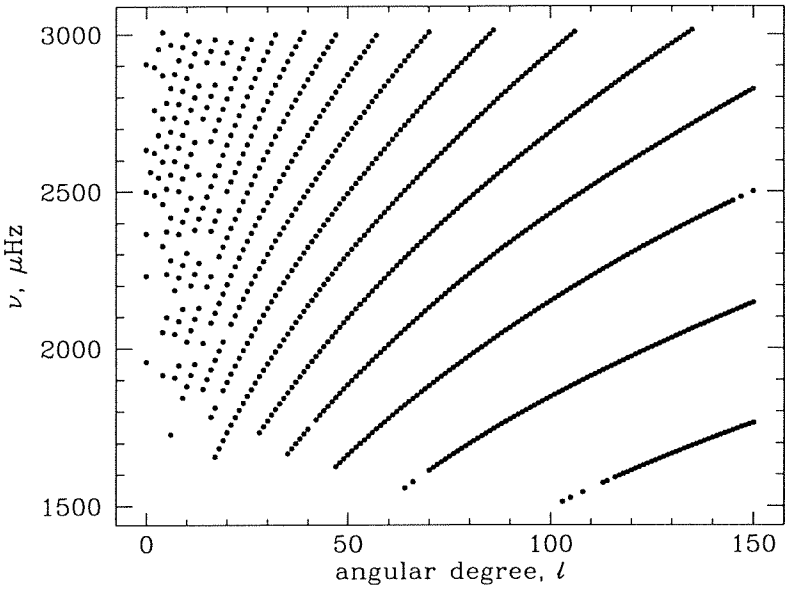

Figure 4: The $l - \nu$ diagram of the solar p modes selected for the Hare-and-Hounds exercise. The gaps in the diagram correspond to the gaps in the initial GONG data, where the frequency measurements were unreliable.

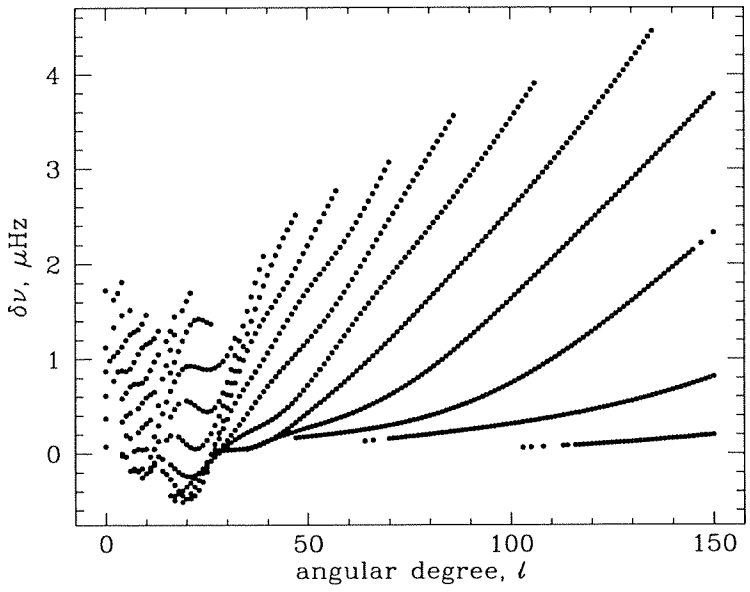

Figure 5: The difference between the frequencies of the proxy and the reference model.

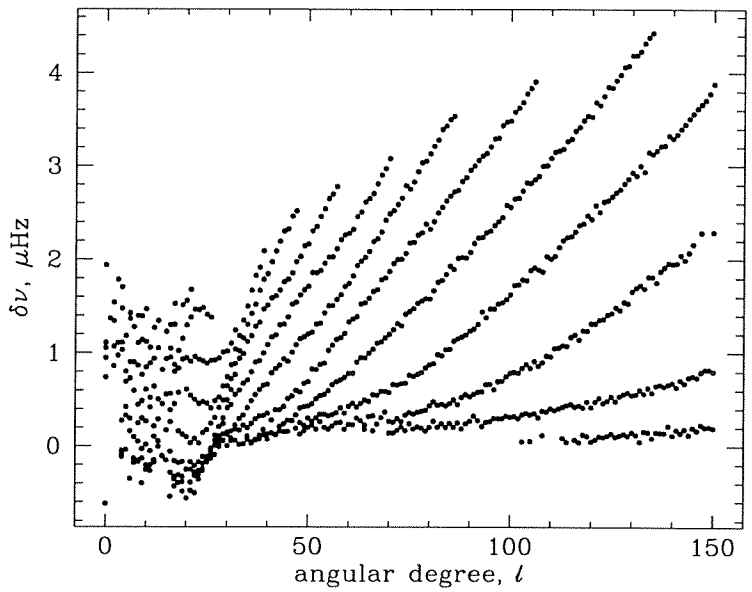

Figure 6: The difference between the frequencies of the proxy with the added noise and the reference model.

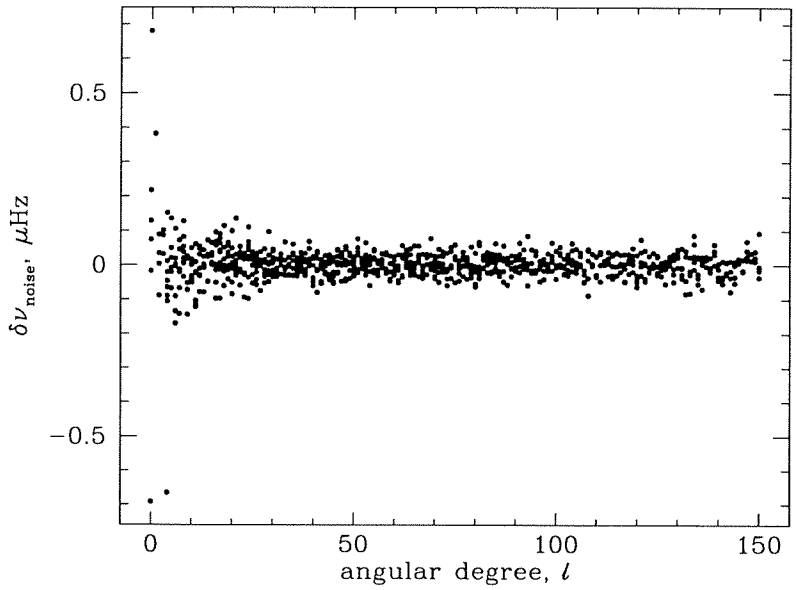

Figure 7: The noise added to the frequencies of the proxy data.

order of 10^{-6}. The data set chosen for the exercise consisted of the frequencies of the p modes of the spherical harmonic degree from 0 to 150 in the frequency range from 1.5 to 3 mHz (Fig. 4). The frequencies of these modes are least affected by the poorly determined upper convective boundary layer and by other non-adiabatic effects. The modes have a sufficiently long life time, and are reliably resolved in the observed power spectra. The same set of modes was used by Gough *et al.* (1996) for inferring the internal structure of the Sun from the initial GONG data. Figure 5 shows the relative frequency difference between the models as a function of the angular degree, l.

The errors added to the frequencies of the proxy model were random numbers computer-generated for the Gaussian distribution with zero mean and the standard deviation corresponding to 1σ standard error estimated from the initial GONG data (Hill *et al.*, 1996). The perturbed frequencies and the errors are shown in Figures 6 and 7, respectively.

Unlike the previous Hare-and-Hounds exercises, neither eigenfunctions nor seismic kernels were provided. Thus, this exercise provided a comprehensive test for the numerical inversions.

4 Results

The test data set was sent by A.G. Kosovichev on 27 January 1996 to groups of inverters who responded to the GONG announcement of 22 December 1995 about the analysis of the initial GONG data and publication of the results. The groups were: D.O. Gough and J.R. Elliott (University of Cambridge), S. Basu and J. Christensen-Dalsgaard (Aarhus University), and H.M. Antia (Tata Institute for Fundamental Research). The groups carried out the test inversion and reported the results which are summarized and compared below with the actual properties of the proxy.

4.1 Sound Speeds

The inversions were carried out for both the adiabatic sound speed, c_S, ($c_S^2 = \gamma p/\rho$) and for the isothermal sound speed, c_T, ($c_T^2 \equiv u = p/\rho$). The second helioseismic variable, in the first case, was density ρ; and, in the second case, the second variable was the helium abundance, Y. Thus, the inversions for the isothermal sound speed involved the equation of state as an additional constraint, whereas the inversions for c_S were independent of the equation of state. We note that the u inferred from the data may be affected by the inaccuracies in the equation of state. However, there are some benefits in constraining the variations of the adiabatic exponent, γ, particularly, in the radiative core where γ is almost constant and equal to 5/3, and of using the $u - Y$ pair of the helioseismic variables. Firstly, u provides resolution better than c_S in the central core, and, secondly, Y provides a direct estimate of the helium abundance in the convection zone. Comparing the results of inversion for c_S^2 and u, one could estimate the accuracy of the equation of state. Often, it was assumed that the variations of γ in the radiative

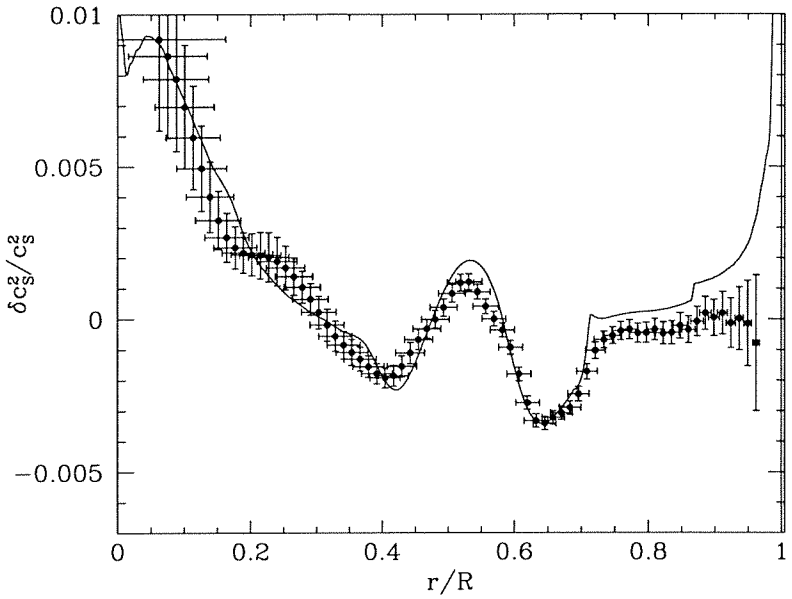

Figure 8: The result of inversion for the sound speed variation by S. Basu and J. Christensen-Dalsgaard (crosses) and the actual variation (solid curve). The horizontal bars show a half-width of the averaging kernels; the vertical bars show the estimated errors.

zone, where the plasma is almost ideal and fully ionized, could be neglected. However, with the new high-precision helioseismic data and solar models, the variations of γ in the radiative zone which are of the order of 10^{-3} become significant.

S. Basu and J. Christensen-Dalsgaard used the technique of Subtractive Optimally Localized Averages (SOLA) [c.f., Pijpers & Thompson 1992]. They carried out inversions for the adiabatic sound speed, c_s, using the density, ρ as the second helioseismic variable, and also inferred the isothermal sound speed, u, using the equation of state as an additional constraint.

H.M. Antia implemented a Regularized Least Squares (RLS) method with iterative refinement [c.f., Antia 1996]. All his inversions were done using ρ and γ as the two independent variables and all other dynamical quantities were computed by assuming hydrostatic equilibrium to produce a complete seismic model. This seismic model was then used as the reference model in subsequent iterations to check for convergence.

The results of the inversions shown in Figures 8-13 are generally in good agreement with the actual difference between the proxy and the reference models. Small deviations of the order of 10^{-3} that exceed the estimated errors are seen in the regions of relatively rapid variation of the first derivatives of $\delta c_S^2/c_S^2$ and $\delta u/u$, that is at $0.4R$, $0.5R$, at the base of the convection zone, and near the surface. Obviously, these deviations partly result from averaging the solar properties around the target points in the inversions.

It is interesting that both groups of inverters detected a small jump in the sound

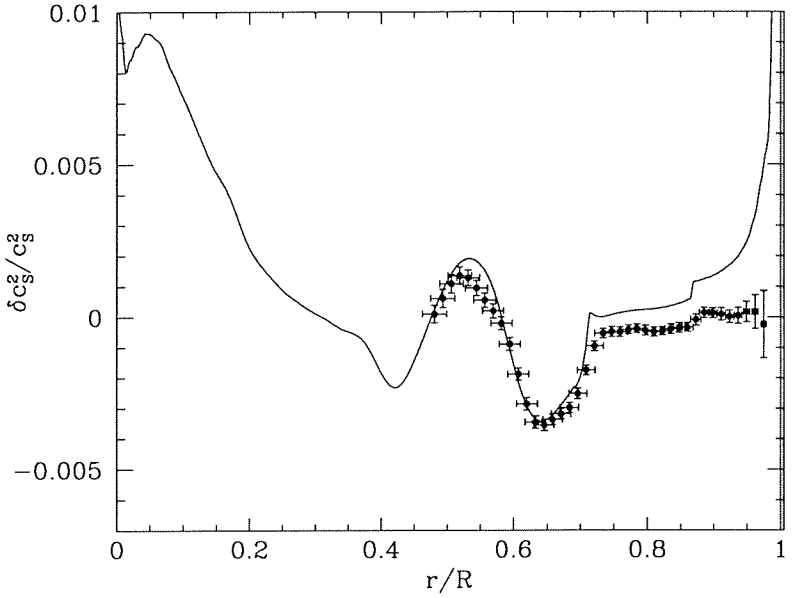

Figure 9: The same as in Fig. 8, but with narrower averaging kernels.

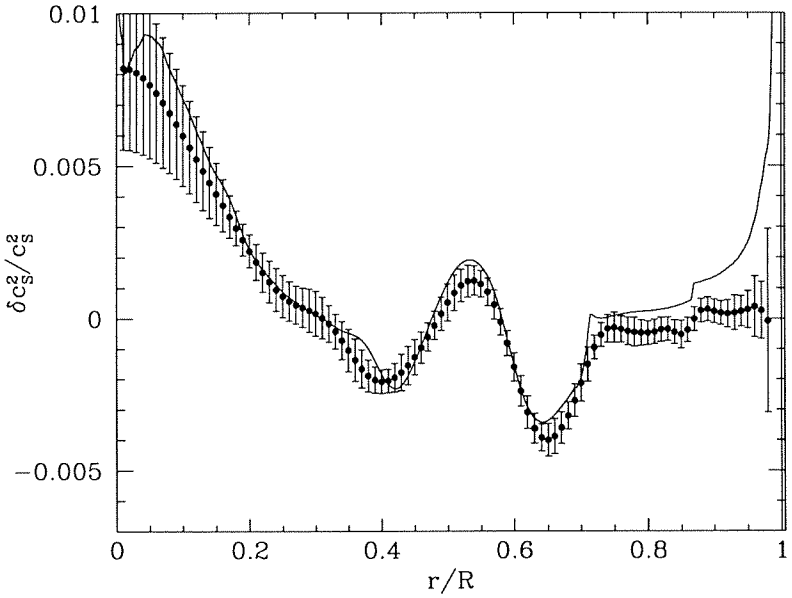

Figure 10: The result of inversion for the sound speed variation by H.M. Antia (points with the error bars), and the actual difference (solid curve).

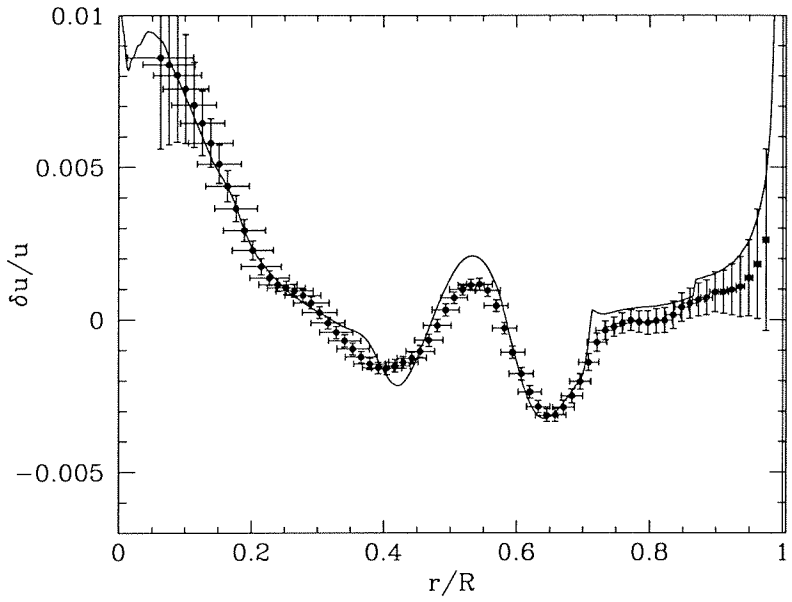

Figure 11: The result of inversion for the variation of u ($\equiv p/\rho$) by S. Basu and J. Christensen-Dalsgaard (crosses) and the actual variation (solid curve). The horizontal bars show a half-width of the averaging kernels; the vertical bars show the estimated errors.

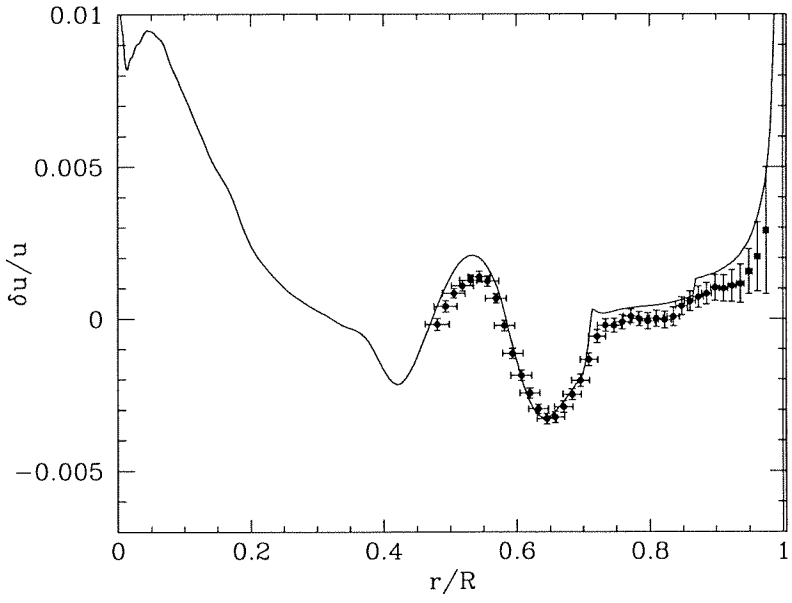

Figure 12: The same as in Fig. 11, but with narrower averaging kernels.

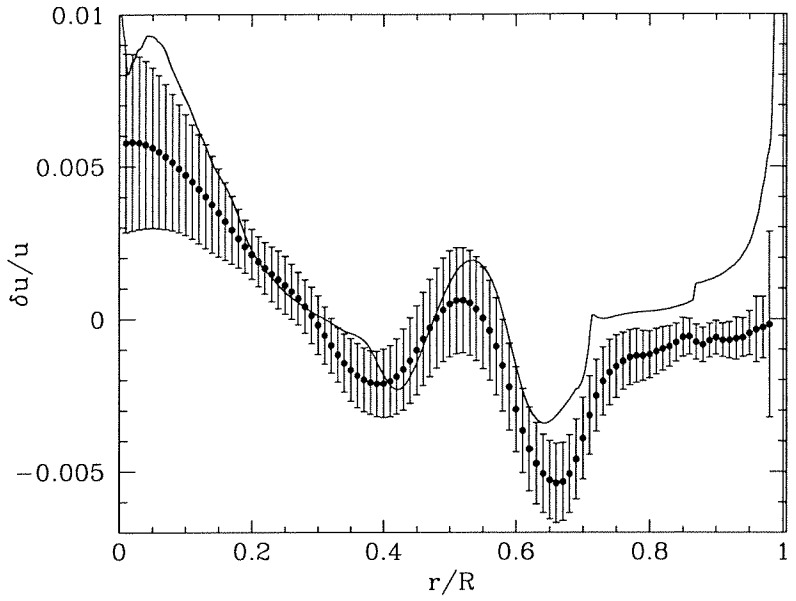

Figure 13: The result of inversion for the variation of u ($\equiv p/\rho$) by H.M. Antia (points with the error bars), and the actual difference (solid curve).

speed of the amplitude of $\approx 5 \times 10^{-4}$ at $r \approx 0.86R$. This jump was a numerical artifact, and had no physical meaning. Nevertheless, its successful detection demonstrates the ability to resolve fine variations of the internal structure of the Sun by using the inversion techniques.

It is also interesting to note that the inversions for u by the SOLA technique (Figures 11 and 12) are more accurate than the inversions for c_S^2 (Figures 8 and 9), whereas, for the RLS technique, the results for c_S^2 are considerably more accurate than the results for u. This is, most likely, a result of using the equation of state as an additional constraint for the SOLA inversions for u. We note that both the proxy and the reference model were computed with the same model of the equation of state (OPAL). Therefore, the uncertainties in the estimates of u caused by an imprecise knowledge of the equation of state were not present.

4.2 Density

The results for the density inversion were provided by S. Basu and J. Christensen-Dalsgaard (Fig. 14) and H.M. Antia (Fig. 15).

S. Basu and J. Christensen-Dalsgaard inferred the density profile using the SOLA technique and the equation of state to constrain the variations of γ. The inversion results by H.M. Antia, who used the RSL method without additional constraints, were independent of the equation of state. The formal errors of his inversion are substantially larger than the errors estimated by S. Basu and J. Christensen-Dalsgaard. This is,

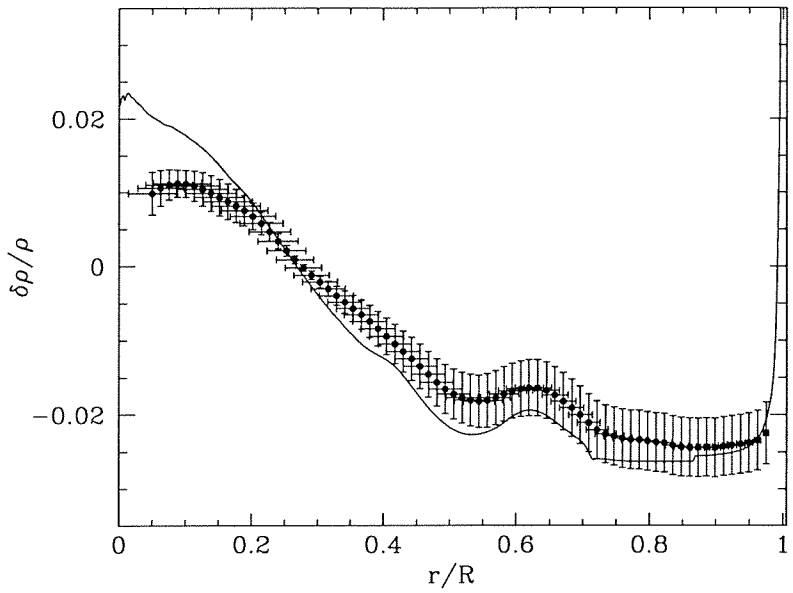

Figure 14: The result of inversion for the density variation by S. Basu and J. Christensen-Dalsgaard (crosses) and the actual variation (solid curve). The horizontal bars show a half-width of the averaging kernels; the vertical bars show the estimated errors.

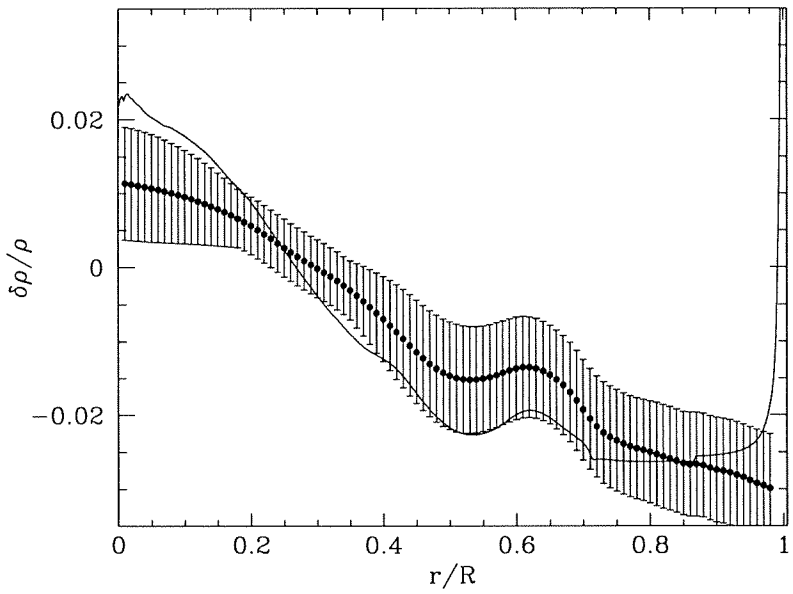

Figure 15: The result of inversion for the density variation by H.M. Antia (points with the error bars), and the actual difference (solid curve).

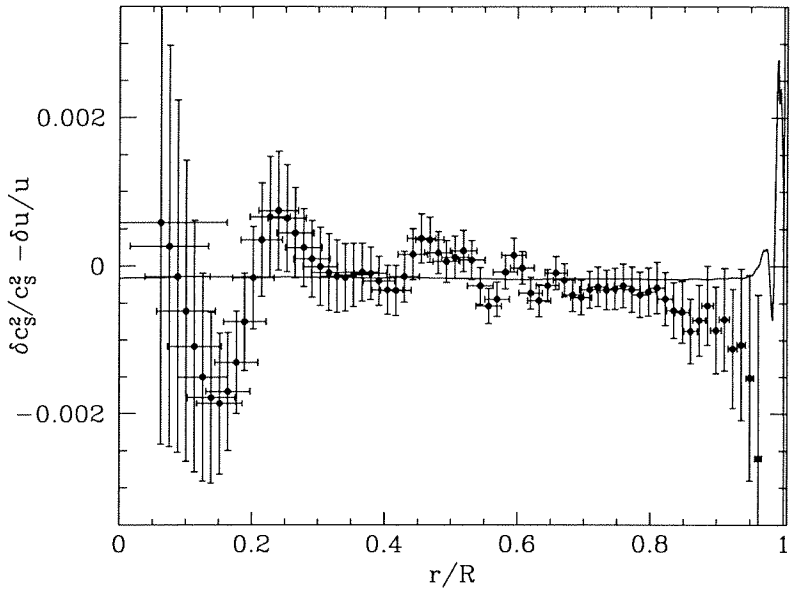

Figure 16: The difference between the variations of c_S^2 and u from the results by S. Basu and J. Christensen-Dalsgaard (crosses), and the actual difference (solid curve)

probably, again the effect of the additional constraint. The density inversions are in reasonable agreement with the actual difference. However, the density estimates are considerably less accurate than the estimates of the sound speed. This is not surprising because asymptotically, in the high-frequency limit, p-mode frequencies depend only on the sound speed. The inverters reported that the accuracy of the density estimates is improved if a broader range of mode frequencies is used in the inversions.

4.3 Adiabatic Exponent

The adiabatic exponent, γ, is an important property of the interior structure. In the solar models, it is determined from the equation of state, the physics of which have not been fully understood. The solar plasma is almost an ideal gas with $\gamma \approx 5/3$ everywhere but the ionization zones. However, the helioseismic inversions are capable, in principle, of detecting the variations of γ not only in the subsurface ionization zones, but also in the deep interior where the non-ideal effects are of the order of 10^{-3}.

The inversions for γ were carried out by H.M. Antia (Fig. 17) and by J.R. Elliott and D.O. Gough (Fig. 18). S. Basu and J. Christensen-Dalsgaard did not determine γ explicitly; however, the difference between their inversions for the adiabatic and isothermal sound speeds plotted in Fig. 16 could result from variations of γ.

H.M. Antia estimated the variations of γ through out the Sun, using ρ as the second helioseismic variable, whereas J.R. Elliott and D.O. Gough concentrated on the variations of γ in the convection zone assuming that the convection zone is adiabatically

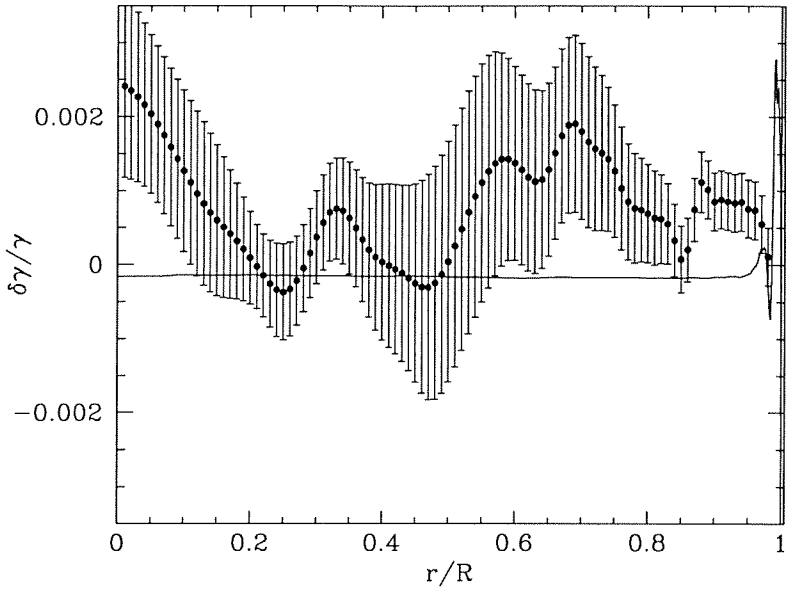

Figure 17: The result of inversion for the adiabatic exponent, γ, by H.M. Antia (points with the error bars), and the actual variation (solid curve).

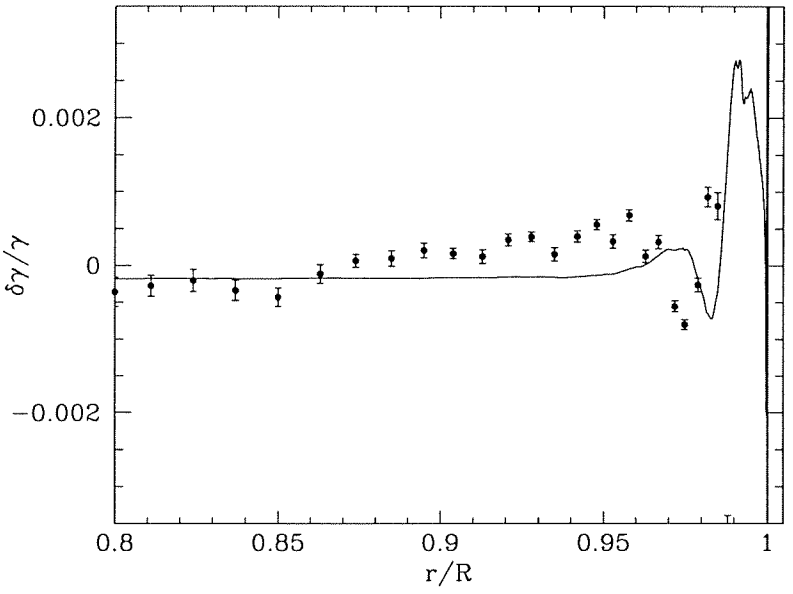

Figure 18: The result of inversion for the variation of the adiabatic exponent, γ, by J.R. Elliott and D.O. Gough (points with the error bars), and the actual variation (solid curve).

stratified. Because of the additional constraint, the estimates by J.R. Elliott and D.O. Gough are more precise than the others. However, evidently, the inversions for γ are not yet reliable.

4.4 Parameter of Convective Stability

The variations of the parameter of convective stability, $A \equiv (1/\gamma)(d\log p/d\log r) - (d\log \rho/d\log r)$, were inferred by H.M. Antia from his inversions for ρ and γ. The result is in good agreement with the actual difference (Fig. 19) demonstrating that the parameter of convective stability can be reliably measured seismologically. This parameter is important, for instance, for predicting the periods of g modes and for studying the convective properties near the base of the convection zone.

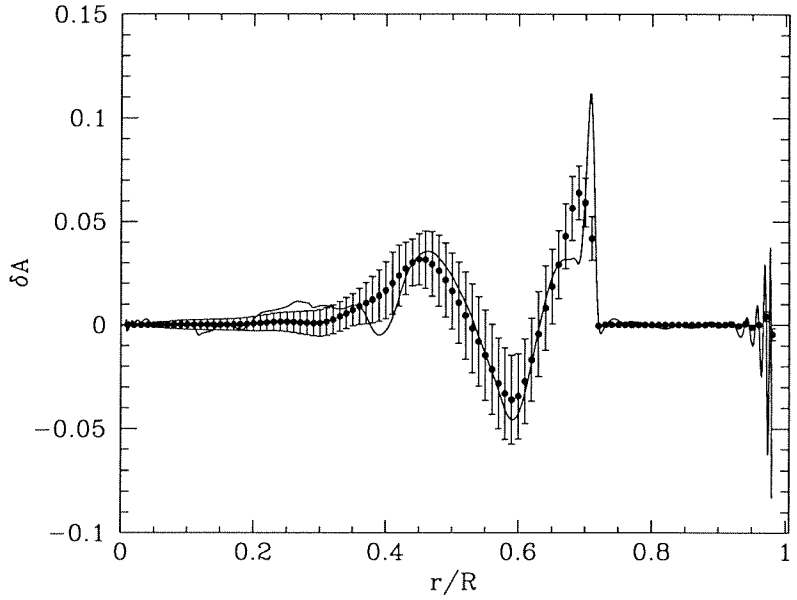

Figure 19: The result of inversion for the variation of the parameter of convective stability, A, by H.M. Antia (points with the error bars), and the actual variation (solid curve).

4.5 Temperature and Helium Abundance in Radiative Zone

H.M. Antia also estimated the variations of the temperature and the helium abundance in the radiative zone using the technique described by Antia and Chitre (1995) (Figures 20 and 21). These results did not agree with the actual difference. One of the reasons for the discrepancy could be that the helium abundance profile in the proxy was not monotonic, but, in the inversions, it was assumed that $Y(r)$ is a monotonic function.

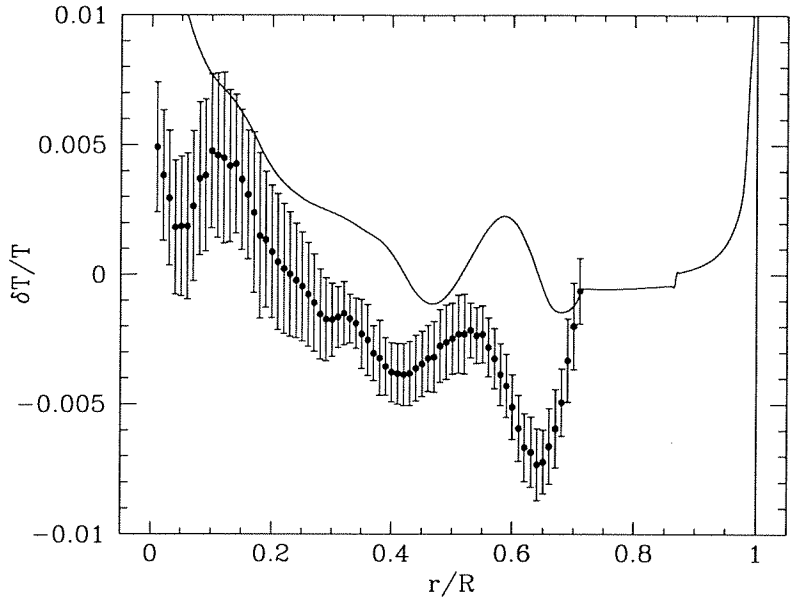

Figure 20: The result of inversion for the temperature variation, T, by H.M. Antia (points with error bars), and the actual variation (solid curve).

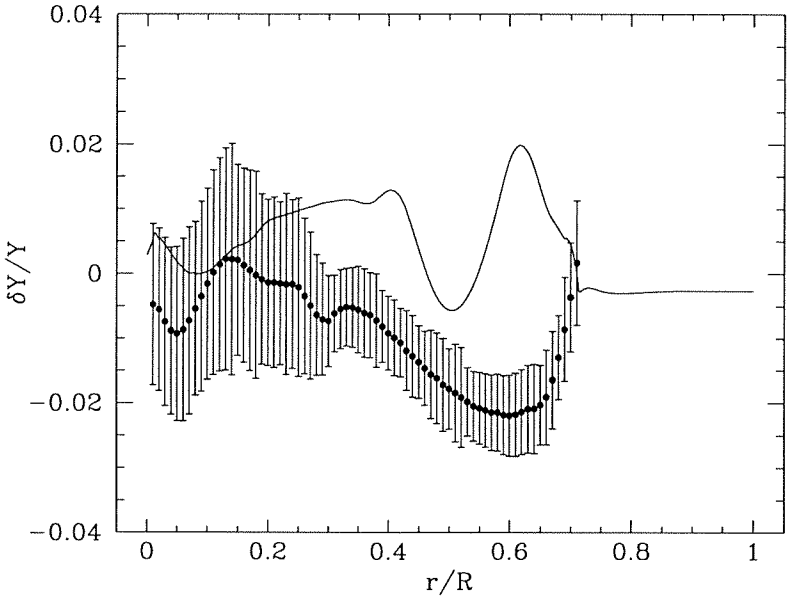

Figure 21: The result of inversion for the helium abundance, Y, by H.M. Antia (points with error bars), and the actual variation (solid curve).

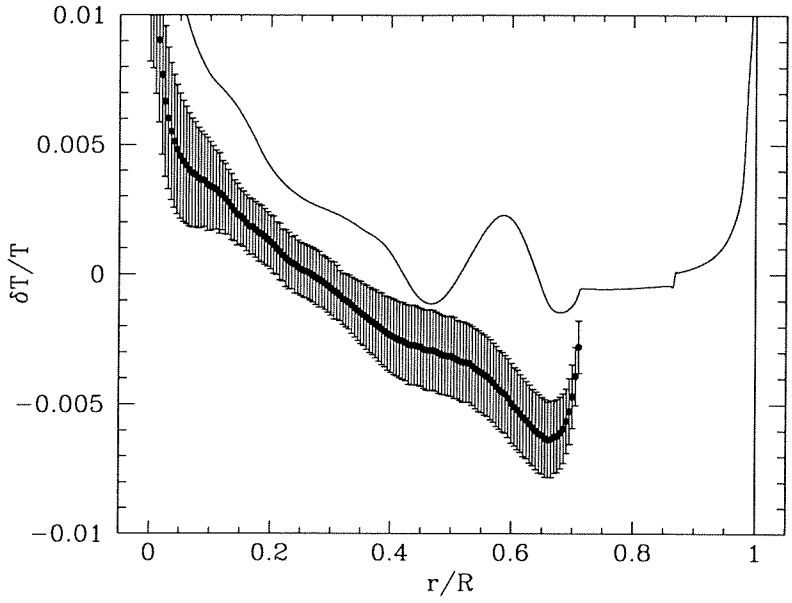

Figure 22: The result of improved inversion for the temperature variation, T, by H.M. Antia (points with error bars), and the actual variation (solid curve).

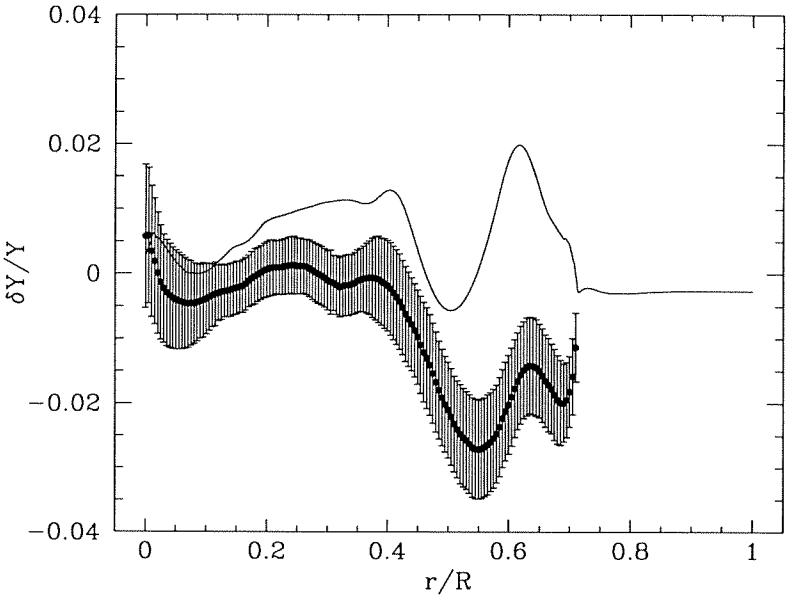

Figure 23: The result of improved inversion for the helium abundance, Y, by H.M. Antia (points with error bars), and the actual variation (solid curve).

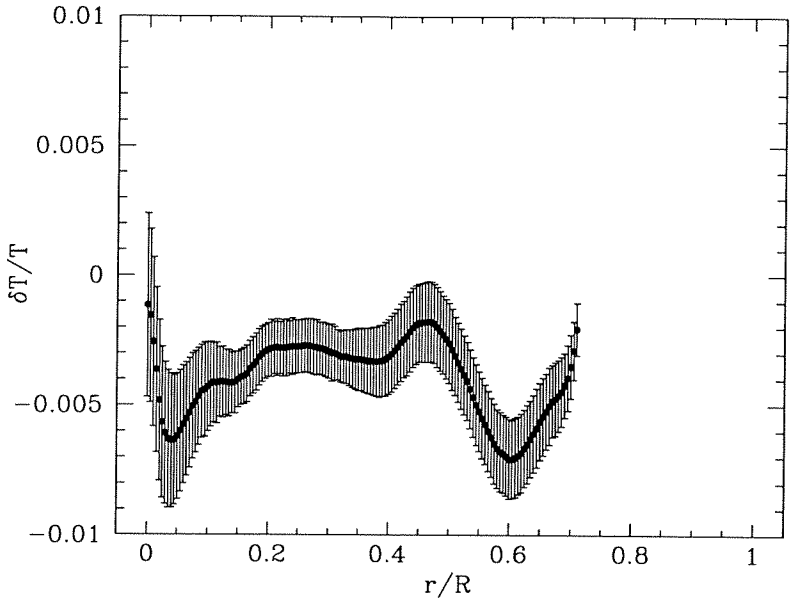

Figure 24: The relative difference between the temperature, T, inferred by H.M. Antia using the technique by Antia and Chitre (1996) and the actual temperature of the proxy.

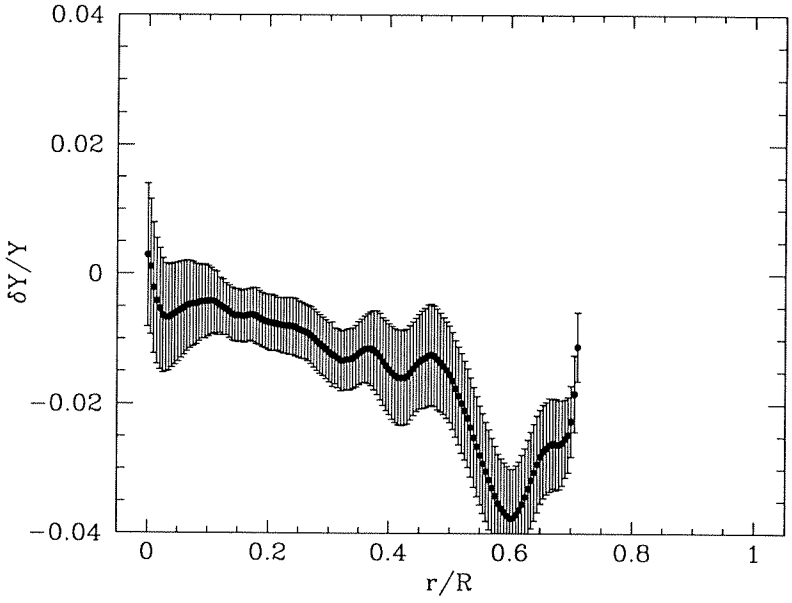

Figure 25: The relative difference between the helium abundance, Y, inferred by H.M. Antia using the technique by Antia and Chitre (1996) and the actual helium abundance of the proxy.

The technique for inferring T and Y was considerably improved by Antia and Chitre (1996) after the Hare-and-Hounds exercise was completed. The new results are shown in Figures 22-25.

5 Conclusions

The Hare-and-Hounds exercise has demonstrated numerically robust structure inversions for both the adiabatic and isothermal sound speeds. The most accurate results were obtained for the squared isothermal sound speed, u ($\equiv p/\rho$) using the optimally localized averages technique and the equation of state to constrain the variations of the adiabatic exponent. Without the additional constraint, the most accurate results were obtained for the adiabatic sound speed by the regularized least squares technique. The estimates of the density and the parameter of convective stability are less accurate than the estimates of the sound speeds. The variations of the adiabatic exponent, the temperature and the helium abundance in the radiative zone were not determined reliably. Additional constraints, such as the equation of state and the equations of thermal balance, are important for improving the accuracy, resolution, and the diagnostic power of the structure inversions. Understanding the physics of the constraints theoretically and seismologically is essential for making robust inferences about solar properties by inversion.

References

[1] Antia, H.M. 1996, Astron. & Astrophys., 308, 656.

[2] Antia, H.M. and Chitre, S.M. 1995, Ap.J., 442, 434.

[3] Antia, H.M. and Chitre, S.M. 1996, preprint.

[4] Bahcall, J.N. and Pinsonneault, M. 1995, Rev. Mod Phys., 67, 781.

[5] Burgers, J.M., 1969, in Flow Equations for Composite Gases, New York: Academic Press.

[6] Caughlan, G.R. and Fowler, W.A., 1988, in: Atomic and Nuclear Data Tables 40, 283

[7] Christensen-Dalsgaard, J. et al. 1996, Science, 272, 1286.

[8] Cox, A.N., Guzik, J.A. and Kidman, R.B. , 1989, ApJ, 342, 1187

[9] Gough, D.O. et al. 1996, Science, 272, 1296.

[10] Guzik, J.A., Cox, A.N. and Swenson, F.J., 1996, Bull Astr. Soc. India, 24, 161.

[11] Hill, F. et al. 1996, Science, 272, 1292.

[12] Michaud, G. and Proffitt, C.R. 1993, in *Inside the Sun*, ed A.Baglin and W.W.Weiss, PAS

[13] Pijpers, F.P. and Thompson, M.J., 1992, Astron. Astrophys., 262, L33

[14] Rogers,F.J. and Iglesias, C., 1992, Ap.J., 401, 361.

[15] Unno, W. et al., 1989, Nonradial Oscillations of Stars, Tokyo: University of Tokyo Press.